Volume 8, Number 3, 2015. pp. 149-155

Jordan Journal of Physics

ARTICLE

On the Distribution of Massive White Dwarfs and Its Implication for Accretion-Induced Collapse

Ali Taani

Physics Department, Faculty of Science, Al-Balqa' Applied University, P.O. Box 1199, 77110 Salt, Jordan.

Physics department, University of Sharjah, P. O. Box 27272 Sharjah, United Arab Emirates.

Received on: 5/1/2015; Accepted on: 7/6/2015

Abstract: A White Dwarf (WD) star and a main-sequence companion may interact through their different stellar evolution stages. This sort of binary population has historically helped us improve our understanding of binary formation and evolution scenarios. The data set used for the analysis consists of 115 well-measured WD masses obtained by the Sloan Digital Sky Survey (SDSS). A substantial fraction of these systems could potentially evolve and reach the Chandrasekhar limit, and then undergo an Accretion-Induced Collapse (AIC) to produce millisecond pulsars (MSPs). I focus my attention mainly on the massive WDs ($M_{WD} \geq 1M_{\odot}$), that are able to grow further by mass-transfer phase in stellar binary systems to reach the Chandrasekhar mass. A mean value of $M \sim 1.15 \pm 0.2M_{\odot}$ is being derived. In the framework of the AIC process, such systems are considered to be good candidates for the production of MSPs. The implications of the results presented here to our understanding of binary MSPs evolution are discussed. As a by-product of my work, I present an updated distribution of all known pulsars in Galactic coordinates pattern.
Keywords: Stars; Neutron stars; White dwarfs; X-ray binaries; Fundamental parameters.

Introduction

Standard stellar evolution models predict that all main-sequence stars in our galaxy with a mass lower than $10M_{\odot}$ will end their lives as white dwarfs (WD), which represent more than 97% of all stars in the galaxy. Because their structural and evolutionary properties are relatively well understood, the characteristics and the physical parameters of WD populations can be used to constrain the evolutionary models and assess the amount of mass, which was lost by their progenitor stars due to the stellar evolution process [1-2]. We only know of a few confirmed examples of very massive WDs ($> 1.2\ M_{\odot}$). Those binary systems are of particular interest because a small amount of accreted mass could drive them above the Chandrasekhar limit, beyond which they become gravitationally unstable [3]. Sloan Digital Sky Survey1 (SDSS) has provided us with a very large sample of WD/main-sequence (WDMS) binaries [4]. This survey allowed us to make a meaningful contribution in terms of the pulsar production. One needs to implement the accretion-induced collapse (AIC) of a WD, which may lead to the formation of a proto neutron star [5 – 8]. This process represents a path alternative to thermonuclear disruption of accreting WDs in Type Ia supernovae (SNe). The scenario for O-Ne-Mg WD begins once the nuclear reaction starts at the center, the burning propagates throughout the entire star and the ignition occurs in the interior. The burning that propagates outward makes central temperatures and pressures high enough to lead instead to a collapse of the WD and induce the contraction of the star. This continues until it reaches the

Corresponding Author: Ali Taani **Email**: ali82taani@gmail.com , ali.taani@bau.edu.jo

Chandrasekhar limit, and finally the star collapses homogeneously leading to the formation of a neutron star. Consequently, the AIC can be a significant contribution to the total number and evolution of low mass X-ray binaries [9]. In the AIC scenario, the explosion energy is expected to be small (10^{49} erg s^{-1}) and the resulting dim and short-lived, making it hard to detect by electromagnetic means [10] and neutrino means alone [11]. Gravitational-wave observations may provide crucial information necessary to reveal a potential AIC. On the other hand, the coalescence of double CO WDs of which the total mass exceeds the Chandrasekhar limit is also likely to end in a collapse induced by electron capture to form a rapidly rotating neutron star, rather than an SNe Ia [12]. However, the nature of the Type Ia progenitors, as well as their precise explosion mechanism, remain a subject of active investigation, both observationally as well as theoretically [13 – 14]. In either AIC or a WD-WD merger, the WD will be rapidly rotating prior to collapse and must eject a sizable fraction of its mass (~0.1 - 0.2 $M_{\odot}$) into a disk during the collapse in order to conserve angular momentum [15, 7].

The Observed Population of WDs

Our present study of SDSS has the following aspects. First, the large and more homogeneous sample of SDSS 2, now available, allows us to test for possible dependencies of the formation and evolution of WD on the stellar masses at the onset of common envelope evolution. Second, I select the sample of massive WDs in binary systems in the range of $M \geq 1M_{\odot}$ (which is considered a relatively small number) causing a higher accretion rate onto the WD, which can reach the Chandrasekhar limit. Finally, the star collapses homogeneously, leading to the formation of a rapidly rotating pulsar. Potential biases affecting the SDSS sample have been analyzed with respect to the WD mass distribution [16]. The sample of WDs analyzed here consists of 115 sources (see Table 1). Fig. 1 shows the Gaussian distribution with mean at $M_{WD} \sim 1.15M_{\odot}$, where the median mass of these sources is $M_{WD} = 1.181 \pm 0.16M_{\odot}$. Furthermore, the knowledge of this distribution is therefore fundamental to understanding the mechanisms involved in the final stages of stellar evolution. I fit the Gauss function to the mass distributions. The Gauss function I chose reads:

$$y = y0 + \frac{A}{w0\sqrt{\frac{\pi}{2}}} \exp\left(-2\left(\frac{x - x0}{w0}\right)^2\right) \quad (1)$$

where y_0, x_0, w_0 and A are offset of y-axis, center of x-axis, width and area represented by the curve, respectively. The value of R (correlation coefficient) expresses the quality of the fitted result. The fitting results are listed in Table 2. It is noteworthy to mention here that the AIC process leads to millisecond pulsar (MSP) with mass less than Chandrasekhar limit [17] and the binding energy also increases; this effect is significant in the estimation of the amount of mass accretion [15]. If matter is accreted at a rate of $M_{\odot} \sim 10^{16} gs^{-1}$ [18] and the total mass accreted exceeds a critical value $\Delta M_{crit} \sim 0.1 - 0.2M_{\odot}$ within 10^9 yrs, then the massive WD will be recycled to become an MSP after the mass reaches the Chandrasekhar limit. One can consider an estimate of the amount of gravitational binding energy (mass loss), due to the conversion from O-Ne-Mg WD matter to MSP. Let us begin with the magnitude of the gravitational potential energy in NS [19]:

$$E = \frac{GM^2}{R} \quad (2)$$

where G is the gravitational constant, M the mass of the companion, R the NS radius.

$$E = \left(\frac{2GM}{c^2}\right)\frac{Mc^2}{2R} \rightarrow \frac{R_S Mc^2}{2R} \quad (3)$$

where R_S is Schwartzchild radius ($R_S = 2GM/c^2 \sim 3$ km for ($M = 1M_{\odot}$)).

$$E = \eta Mc^2 \quad (4)$$

where $\eta = R_S/2R$, thus:

$$E \sim 0.1Mc^2. \quad (5)$$

As a result, around 10% of mass will go as binding energy and reduce the mass of the amount $1.4M_{\odot}$ by about $0.14M_{\odot}$, where the total energy is:

$$Mc^2(1-\eta). \quad (6)$$

This effect is significant in the estimation of the amount of accreted mass. However, unfortunately, most of the studies argued that the binding energy of the NS is not commonly considered [15]. More modeling is required to support such a conclusion.

TABLE 1. Parameters of binary systems of WDs with compact companions. Data were taken from SDSS catalogue.

IAU Name	$M_{wd}(M_\odot)$	Errors $M_{wd}(M_\odot)$	$M_{seccandary}(M_\odot)$	$E_{rros}M_{sec}(M_\odot)$	$R_{wd}(R_\odot)$
SDSSJ001247.18+001048.7	1.23	0.442	0.38	0.072	0.00538
SDSSJ001855.19+002134.5	1.24	0.391	0.38	0.072	0.00526
SDSSJ002157.90-110331.6	1.08	0.051	0.319	0.09	0.0071
SDSSJ002959.94+001132.7	1.15	0.386	0.431	0.1	0.00637
SDSSJ003301.53+005716.9	1.19	0.286	0.38	0.072	0.00588
SDSSJ003643.33+252754.9	1	0.113	0.118	0.004	0.00807
SDSSJ003731.07+010947.0	0.98	0.629	0.319	0.09	0.00826
SDSSJ004511.95+250330.9	1.13	0.037	0	0	0.00654
SDSSJ004604.14+011037.4	1.16	0.386	0.464	0.088	0.00618
SDSSJ005245.11-005337.2	1.26	0.365	0.319	0.09	0.00502
SDSSJ011634.11+002956.5	0.93	0.348	0.319	0.09	0.00898
SDSSJ013504.31-085919.0	1.23	0.222	0.319	0.09	0.00538
SDSSJ015434.31-010611.1	0.98	0.688	0.255	0.124	0.00818
SDSSJ015657.37-003341.6	0.91	0.357	0.464	0.088	0.0093
SDSSJ020925.74+064213.9	1.15	0.15	0.319	0.09	0.00644
SDSSJ021309.19-005025.4	1.02	0.423	0.38	0.072	0.00779
SDSSJ024642.55+004137.2	0.95	0.099	0.38	0.072	0.00873
SDSSJ024645.89-010624.1	1.31	0.355	0.38	0.072	0.0044
SDSSJ030351.97+003548.4	1.307	0.281	0.431	0.1	0.00448
SDSSJ030904.82-010100.8	0.977	0.406	0.355	0.072	0.00846
SDSSJ031206.82-002145.4	1.13	0.651	0.319	0.09	0.00654
SDSSJ032656.44+002232.1	1.105	0.447	0.431	0.1	0.00694
SDSSJ033804.40+002740.3	1.37	0.091	0	0	0.0038
SDSSJ035912.46-044630.2	1.24	1.058	0.38	0.072	0.00525
SDSSJ052624.54+621344.2	1.07	0.037	0.38	0.072	0.00723
SDSSJ073250.34+393633.9	0.905	0.074	0	0	0.00917
SDSSJ074207.89+275845.1	1.385	0.054	0.319	0.09	0.00355
SDSSJ075325.93+164132.7	1.19	0.411	0.464	0.088	0.00581
SDSSJ080304.61+121810.3	1.04	0.274	0.431	0.1	0.00768
SDSSJ080653.95+160729.8	0.91	0.269	0.38	0.072	0.0091
SDSSJ081312.09+324758.6	0.9	0.204	0.255	0.124	0.00917
SDSSJ081811.70+173224.5	1.04	0.173	0.38	0.072	0.00768
SDSSJ081831.07-010923.1	1.14	0.311	0.38	0.072	0.00648
SDSSJ083722.44+265417.3	0.94	0.065	0.319	0.09	0.00877
SDSSJ083827.09+415015.5	1.07	0.365	0.464	0.088	0.00723
SDSSJ083920.48+125959.5	1.12	0.154	0.118	0.004	0.0066
SDSSJ084009.24+281201.9	1.07	0.262	0.38	0.072	0.00756
SDSSJ084056.91+275513.7	1.07	0.203	0.38	0.072	0.0073
SDSSJ084307.27+122610.1	0.95	0.129	0.196	0.085	0.0086
SDSSJ084400.82+052305.7	0.94	0.284	0.319	0.09	0.00893
SDSSJ085847.47+371115.5	1.03	0.366	0.464	0.088	0.00849
SDSSJ091143.09+222748.8	1.46	0.051	0.38	0.072	0.0027
SDSSJ091309.70+223346.7	0.98	0.167	0.431	0.1	0.00828
SDSSJ092200.71+181714.1	1.02	0.187	0.38	0.072	0.0078
SDSSJ092313.99+205119.9	1.16	0.18	0.38	0.072	0.00623
SDSSJ092433.98+204020.0	1.04	0.113	0.319	0.09	0.00754
SDSSJ093236.83+053026.6	1.02	0.16	0.464	0.088	0.0078
SDSSJ093426.60+053753.6	0.93	0.277	0.319	0.09	0.00912
SDSSJ093427.91+204658.6	1.03	0.418	0.196	0.085	0.00759
SDSSJ093526.43+245423.4	1.02	0.224	0.431	0.1	0.00785
SDSSJ093632.33+341932.6	1.03	0.114	0.319	0.09	0.00767

IAU Name	$M_{wd}(M_{\odot})$	Errors $M_{wd}(M_{\odot})$	$M_{seccandary}(M_{\odot})$	$E_{rros}M_{sec}(M_{\odot})$	$R_{wd}(R_{\odot})$
SDSSJ094002.40+534202.9	0.95	0.159	0.255	0.124	0.00868
SDSSJ094542.61+173859.9	1.01	0.185	0.472	0.062	0.00821
SDSSJ094720.94+111734.7	1.12	0.193	0.464	0.088	0.0074
SDSSJ094821.30+365935.3	1.26	0.135	0.38	0.072	0.00501
SDSSJ094952.73+012603.4	1.14	0.248	0.319	0.09	0.00648
SDSSJ100015.18+304330.5	0.93	0.214	0.255	0.124	0.00898
SDSSJ100609.18+004417.0	0.93	0.083	0.118	0.004	0.00879
SDSSJ101006.92+301211.3	1.2	0.158	0.255	0.124	0.00568
SDSSJ101116.29+182749.5	0.92	0.229	0	0	0.00992
SDSSJ101124.31+644655.5	1.15	0.166	0.118	0.004	0.00636
SDSSJ101614.69+490930.3	1.01	0.168	0.319	0.09	0.00801
SDSSJ102213.46+294119.9	1.275	0.315	0.319	0.09	0.00483
SDSSJ104459.32+360554.7	1.24	0.052	0.255	0.124	0.00519
SDSSJ105038.62+413834.5	0.95	0.085	0.196	0.085	0.00861
SDSSJ110736.88+612232.8	1	0.043	0.464	0.088	0.00815
SDSSJ114720.00+112813.3	0.91	0.296	0.464	0.088	0.00909
SDSSJ114913.52-014728.6	0.9	0.057	0.319	0.09	0.00917
SDSSJ120222.10+411810.8	0.97	0.414	0.38	0.072	0.0087
SDSSJ121928.05+161158.7	0.98	0.124	0.196	0.085	0.00818
SDSSJ122634.97+322020.8	1.36	0.108	0.319	0.09	0.00379
SDSSJ122850.46-022509.4	1.18	0.379	0	0	0.00599
SDSSJ122930.65+263050.4	1.04	0.077	0.38	0.072	0.0077
SDSSJ125207.48+444827.8	0.9	0.231	0	0	0.00938
SDSSJ125919.51+321935.4	0.9	0.116	0.38	0.072	0.00915
SDSSJ131156.69+544455.8	1.19	0.036	0.431	0.1	0.0058
SDSSJ132652.62+000855.3	0.97	0.446	0.464	0.088	0.00863
SDSSJ134557.68+330050.6	0.97	0.097	0.464	0.088	0.00839
SDSSJ134714.30+412909.6	1.25	0.142	0.431	0.1	0.00513
SDSSJ135502.75+574058.3	1.46	0.049	0	0	0.0027
SDSSJ142241.90+513537.9	1.23	0.043	0	0	0.00537
SDSSJ143519.16+362952.0	1.02	0.121	0.319	0.09	0.00773
SDSSJ145514.56-022822.2	0.94	0.381	0.149	0.075	0.00866
SDSSJ151714.96+423924.7	1.25	0.02	0.38	0.072	0.00507
SDSSJ151817.97+455334.1	0.97	0.245	0.464	0.088	0.00833
SDSSJ154609.98+200320.6	1.12	0.208	0.464	0.088	0.00674
SDSSJ154928.56+385419.3	0.93	0.222	0.431	0.1	0.00882
SDSSJ155332.86+045735.1	0.91	0.174	0.38	0.072	0.0091
SDSSJ155933.42+340502.5	0.96	0.254	0	0	0.00838
SDSSJ160821.47+085149.9	0.98	0.083	0.196	0.085	0.00826
SDSSJ160824.57+285524.9	1.06	0.286	0.319	0.09	0.00742
SDSSJ161715.27+081849.0	1.02	0.295	0.464	0.088	0.0079
SDSSJ161726.96+385557.5	1.02	0.282	0.319	0.09	0.00807
SDSSJ162324.05+343647.7	0.97	0.071	0.118	0.004	0.00832
SDSSJ170127.36+253302.6	1.01	0.08	0.38	0.072	0.00793
SDSSJ170843.52+215829.0	1.27	0.224	0.464	0.088	0.00502
SDSSJ171145.42+555444.4	0.94	0.04	0.319	0.09	0.01017
SDSSJ171411.14+294508.2	0.91	0.231	0.319	0.09	0.00933
SDSSJ172008.58+565211.8	1.29	0.276	0.464	0.088	0.00471
SDSSJ205059.37-000254.3	0.95	0.099	0.319	0.09	0.00862
SDSSJ205316.52-010616.5	0.9	0.112	0.38	0.072	0.00915
SDSSJ210624.12+004030.2	1.03	0.105	0.464	0.088	0.00774
SDSSJ210751.44+005854.4	1.01	0.268	0	0	0.00811
SDSSJ211132.76+011522.2	0.96	0.124	0.431	0.1	0.00847

IAU Name	$M_{wd}(M_{\odot})$	Errors $M_{wd}(M_{\odot})$	$M_{seccandary}(M_{\odot})$	$E_{rros}M_{sec}(M_{\odot})$	$R_{wd}(R_{\odot})$
SDSSJ211205.31+101427.9	1.06	0.051	0.196	0.085	0.00744
SDSSJ214447.51+004201.5	1.01	0.446	0.149	0.075	0.00785
SDSSJ215744.77-004015.1	1.2	0.345	0.319	0.09	0.00575
SDSSJ220848.99+122144.7	1.24	0.134	0	0	0.00568
SDSSJ224522.42-000109.5	1.11	0.222	0.38	0.072	0.00686
SDSSJ224932.02+000645.7	1.08	0.217	0.196	0.085	0.00709
SDSSJ231014.62+001439.9	1.07	0.32	0.38	0.072	0.00722
SDSSJ232527.81-005416.7	0.93	0.194	0.255	0.124	0.00898
SDSSJ232624.72-011327.2	1.46	0.372	0.38	0.072	0.00269
SDSSJ232816.06+010036.0	1.31	0.931	0.38	0.072	0.00447
SDSSJ234749.84+431424.6	0.99	0.079	0.255	0.124	0.0082
SDSSJ235324.74+351623.2	1.08	0.211	0.255	0.124	0.00709
SDSSJ011355.84-093938.0	1.24	0.156	0.319	0.09	0.00519
SDSSJ041518.90+165238.2	1.28	0.066	0	0	0.00483
SDSSJ042437.67+063408.2	0.92	0.169	0.464	0.088	0.0099
SDSSJ044542.27+120246.7	1.15	0.168	0.255	0.124	0.00635
SDSSJ064411.89+285301.1	0.96	0.122	0	0	0.00936
SDSSJ064715.54+275948.3	1	0.13	0	0	0.00799
SDSSJ085224.02+111520.8	0.93	0.407	0.319	0.09	0.00898
SDSSJ093349.93+151718.5	1	0.125	0.431	0.1	0.00825
SDSSJ100811.87+162450.4	1.23	0.07	0.464	0.088	0.00575
SDSSJ113223.69+225313.1	0.98	0.053	0.464	0.088	0.00845
SDSSJ113511.13+000923.9	0.935	0.157	0.319	0.09	0.00875
SDSSJ125645.47+252241.6	1.01	0.06	0.255	0.124	0.00818
SDSSJ140516.05+232246.9	0.94	0.069	0	0	0.00883
SDSSJ141451.60+193638.9	1.07	0.13	0.196	0.085	0.00716
SDSSJ173430.11+335407.5	1.19	0.133	0.319	0.09	0.00586
SDSSJ213225.96+001430.5	0.92	0.125	0.319	0.09	0.00904
SDSSJ011123.90+000935.2	0.93	0.202	0.431	0.1	0.00899
SDSSJ014232.59-083528.4	1.07	0.05	0.38	0.072	0.00722
SDSSJ025347.51+335221.0	1.02	0.121	0.431	0.1	0.00808
SDSSJ044831.02+214909.8	1.01	0.11	0.38	0.072	0.00793
SDSSJ072130.60+374228.3	0.96	0.102	0.319	0.09	0.00854
SDSSJ072434.72+321609.4	0.98	0.051	0.319	0.09	0.00835
SDSSJ085223.75+071326.0	0.92	0.231	0.319	0.09	0.00896
SDSSJ102102.25+174439.9	1.06	0.087	0.319	0.09	0.00768
SDSSJ112308.40-115559.3	1.26	0.07	0.255	0.124	0.00501
SDSSJ112651.03-081640.1	1.26	0.125	0.431	0.1	0.00501
SDSSJ120953.67+185815.7	0.96	0.126	0.464	0.088	0.00883
SDSSJ130012.49+190857.4	1.09	0.103	0.319	0.09	0.0069
SDSSJ135207.77+185033.8	1.1	0.122	0.38	0.072	0.00684
SDSSJ141052.79+375435.6	1.03	0.074	0.464	0.088	0.00767
SDSSJ142503.62+073846.4	0.97	0.13	0.38	0.072	0.0087
SDSSJ142631.93+091621.1	1.4	0.075	0.38	0.072	0.00343
SDSSJ142951.19+575949.0	1.07	0.131	0.38	0.072	0.0073
SDSSJ143143.83+565728.2	1	0.285	0.255	0.124	0.00799
SDSSJ145305.77+001048.2	0.95	0.054	0.319	0.09	0.00861
SDSSJ153009.49+384439.8	0.92	0.282	0.431	0.1	0.00895
SDSSJ155808.49+264225.7	1.06	0.309	0.319	0.09	0.00736
SDSSJ162354.45+630640.4	1	0.089	0.319	0.09	0.00799
SDSSJ173849.76+635042.0	0.93	0.123	0.38	0.072	0.00898

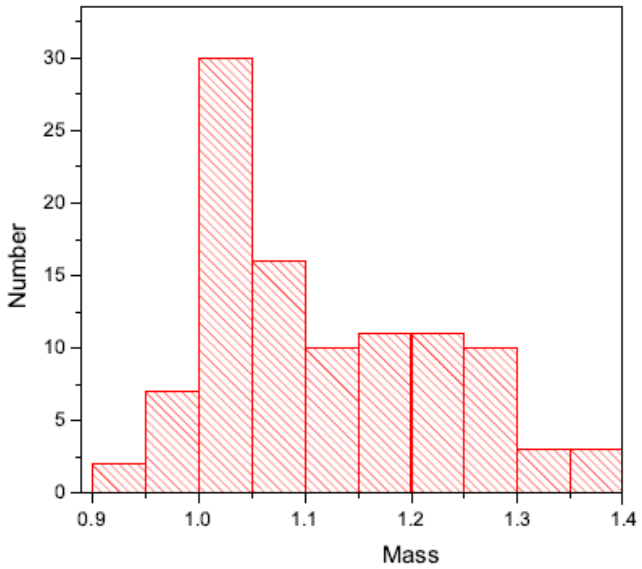

FIG. 1. Histograms of the mass distribution of WDs. The distribution is relatively Gaussian.

TABLE 2. The fitting results of the distribution for mass of WDs.

Quantity	y_0	x_0	w	A	σ	χ^2/Dof	R^2
M_{WDs}	0.53 ± 0.64	0.79 ± 0.012	0.40 ± 0.03	12.30 ± 0.92	0.20	3.311	0.955

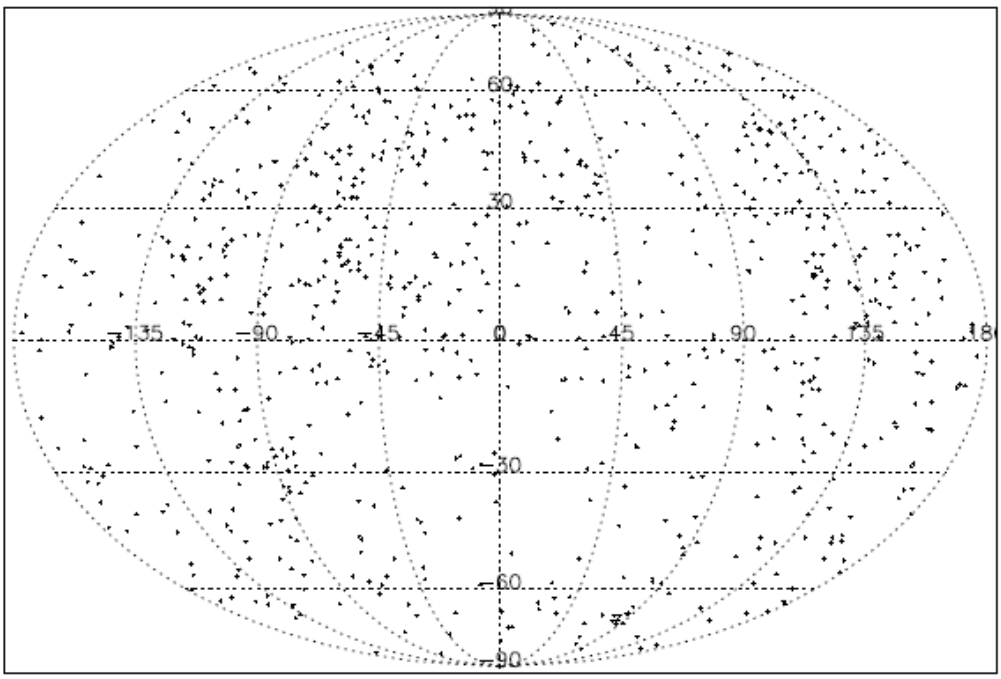

FIG. 2. The full-sky distribution of all known WDs, shown in Galactic coordinates in which the plane of the Galaxy is at the equator and the Galactic center is at the origin. The data are taken from [23].

Fig. 2 shows the spatial density distribution of the current sample of all known WD systems throughout the Galaxy. The scale-height of the WDs is somewhat completed and uniformly distributed.

Summary and Conclusions

Interacting binaries can play an important role in terms of studying the mass transfer and orbital motion of the companions as well as the effects of binary evolution on the final fate of the compact objects and SNe.

In the frame of this process, the AIC scenario to produce binary MSPs must be invoked, since it is expected to turn into normal magnetized rotating neutron stars, which in binaries can evolve into MSPs through the recycling process. In addition, it could provide us with a better match to the period distributions of some types of binary MSPs. One example is the double relativistic pulsar PSR J0737–3039 [20 – 21], and it seems to be an interesting issue requiring further studies for the analysis of the formation of neutron stars in Galactic disk as well as globular clusters. Since the evolution of accreting WDs seriously affects the pulsar production via mass and angular momentum accretion during the AIC scenario, substantial adjustments to the current picture on MSP progenitor population are requires. I will add this clarification and point out possibilities for future research.

Finally, it is worth mentioning here that the most highly magnetized WDs are massive as well as isolated. This depends on the strength of the WD magnetic field. The matter flowing through the inner Lagrangian point (L1) can form either a full or a partial accretion disk [22] or else follow the magnetic field lines down to the surface at the magnetic poles. Thus, it is important to monitor long orbital period of WD systems in order to gain insight into the dynamics and binary evolution of those systems that are most likely to undergo the AIC process.

References

[1] Warner, B. and Woudt, P.A., ASP Conf. Seri., 261 (2002) 406, arXiv: astro-ph/0109397.

[2] Zorotovic, M., Schreiber, M.R., Gänsicke, B.T. and Nebot Gómez-Morán, A., A&A, 520 (2010) 86.

[3] Mereghetti, S., Tiengo, A., Esposito, P., La Palombara, N., Israel, G.L. and Stella, L., Science, 325 (2009) 1222.

[4] Abazajian, K.N., Adelman-McCarthy, J.K., Agüeros, M.A., Allam, S. S. et al., ApJS, 182 (2009) 543.

[5] Nomoto, K., Astrophys. J., 322 (1987) 206.

[6] Taani, A., Zhang, C.M., Al-Wardat, M. and Zhao, Y.H., AN, 333 (2012a) 53.

[7] Taani, A., Zhang, C.M., Al-Wardat, M. and Zhao Y.H., Ap&SS, 340 (2012b) 147.

[8] Tauris, T.M., Sanyal, D., Yoon, S.-C. and Langer, N., A&A, 558A (2013) 39.

[9] van den Heuvel, E.P.J., Science, 303 (2004) 1143.

[10] Darbha, S., Metzger, B.D., Quataert, E., Kasen, D., Nugent, P. and Thomas, R., MNRAS, 409 (2010) 846.

[11] Metzger, B.D., Piro, A.L. and Quataert, E., MNRAS, 396 (2009) 304.

[12] Podsiadlowski, Ph., Langer, N., Poelarends, A.J.T., Rappaport, S., Heger, A. and Pfahl, E., ApJ, 612 (2004) 1044.

[13] Han, Z., ApJ, 677 (2008) L109.

[14] Wang, B. and Han, Z., Ap&SS, 329 (2010) 293.

[15] Bagchi, M., arXiv:1004.2730v2 (2011).

[16] Rebassa-Mansergas, A., Nebot Gómez-Morán, A., Schreiber, M. R., Girven, J. and Gänsicke, B.T., MNRAS, 413 (2011) 1121.

[17] Zhang, C.M., Wang, J., Zhao, Y.H. et al., A&A, 527 (2011) A83.

[18] Zhang, C.M. and Kojima, Y., MNRAS, 366 (2006) 137Z.

[19] Shapiro, S.L. and Teukolsky, S.A., "Black Holes, White Dwarfs and Neutron Stars", 8th Ed. (Wiley, New York, 1983) chapter 14.

[20] Burgay, M., D'Amico, N., Possenti, A., Manchester, R.N., Lyne, A.G., Joshi, B.C., McLaughlin, M.A. et al., Nature, 426 (2003) 531.

[21] Lyne, A.G., Burgay, M., Kramer, M., Possenti, A., Manchester, R.N., Camilo, F., McLaughlin, M.A. et al., Science, 303 (2004) 1153.

[22] Zhang, C.M., Wickramasinghe, D.T. and Ferrario, L., MNRAS, 397 (2009) 2208Z.

[23] Ritter, H. and Kolb, U., A&A, 404 (2003) 301 (update RKcat7.21, 2014) http://www.mpa-garching.mpg.de/RKcat/